

See discussions, stats, and author profiles for this publication at: <https://www.researchgate.net/publication/231370090>

Process Intensification: Precipitation of Barium Sulfate Using a Spinning Disk Reactor

ARTICLE *in* INDUSTRIAL & ENGINEERING CHEMISTRY RESEARCH · SEPTEMBER 2002

Impact Factor: 2.59 · DOI: 10.1021/ie010654w

CITATIONS

58

READS

30

4 AUTHORS, INCLUDING:



Lorenzo Cafiero

ENEA

7 PUBLICATIONS 63 CITATIONS

SEE PROFILE



Angelo Chianese

Sapienza University of Rome

68 PUBLICATIONS 767 CITATIONS

SEE PROFILE

PROCESS DESIGN AND CONTROL

Process Intensification: Precipitation of Barium Sulfate Using a Spinning Disk Reactor

L. M. Cafiero,[†] G. Baffi,[†] A. Chianese,^{*,†} and R. J. J. Jachuck[‡]

Department of Chemical Engineering, University of Rome "La Sapienza" via Eudossiana 18, I-00184 Rome, Italy, and Process Intensification and Innovation Centre (PIIC), Department of Chemical and Process Engineering, University of Newcastle upon Tyne, Newcastle upon Tyne, U.K.

In this work, the use of a spinning disk reactor as a unit for a reaction–precipitation process is investigated. An experimental study is reported concerning the precipitation of barium sulfate from aqueous solutions at 25 °C on a spinning disk of 0.5 m in diameter. At a rotational speed higher than 900 rpm, spontaneous precipitation took place and crystals $\sim 0.7 \mu\text{m}$ in size were produced. At a supersaturation ratio of 2000, the number of generated crystals is comparable with those reported in the literature when a T-mixer is used, but in the case of the spinning disk, a much lower specific dispersed power is required.

Introduction

There is a growing demand for particles with controlled size, shape, and size distribution. More recently, the use of submicrometer-size particles ($\sim 1 \mu\text{m}$ or less) has found great importance in the production of fine chemicals, catalysts, and pharmaceuticals and in electronic applications due to their superior properties. Precipitation from solution represents an inexpensive and simple method for producing nanoparticles of the dimension of a few micrometers or smaller. The size distribution of crystals from precipitation is mainly affected by the first step of the crystallization process, i.e., primary nucleation. At a very high primary nucleation rate, precipitation can reduce the cost of production of nanoparticles and can enhance the quality of the product, in terms of average particle size and particle size distribution.

Precipitation is commonly defined as the crystallization of sparingly soluble substances, which are formed by a chemical reaction. Precipitation phenomena involve the simultaneous and rapid occurrence of different processes. In particular, it is possible to identify a number of primary processes, such as the mixing of the reactants on macro-, meso-, and microscale, the chemical reaction, and the nucleation and growth of the solid particles. In general, the two latter processes happen concurrently to secondary phenomena, such as particle aggregation, aging, and ripening. It is therefore possible to identify primary particles, which are formed by crystal nucleation and growth, and secondary particles, which derive mainly from aggregation phenomena.

Supersaturation is known to play the main role in controlling the mechanism and the kinetics of nucleation

and growth processes. In particular, heterogeneous nucleation can take place at any level of supersaturation within the metastable limits. In this case, the generation of nuclei is catalyzed by foreign particles, typically dust. On the contrary, very high levels of supersaturation are required for homogeneous nucleation, since in this case the critical nucleus can be only generated by the collisions of a high number of solute clusters randomly moving in solution. Depending on the level of supersaturation, nucleation phenomena are generally very fast in precipitation processes (with induction times of $\sim 1 \text{ ms}$). Since the gradient force of the nucleation process is local supersaturation, the intensity of mixing plays a fundamental role in determining the precipitation mechanism and, hence, particle properties and crystal size distribution. Thus, very high levels of supersaturation and intense mixing are required to ensure that homogeneous nucleation is the dominant nucleation mechanism.

In this paper, the use of spinning disk reactors for precipitation processes is presented. Such reactors have been shown to be very effective as continuous-flow mixers.^{1,2} These devices use centrifugal acceleration to produce very thin films on the surface of a rotating disk. As observed by Jachuck and Ramshaw,¹ this has several advantages, including the ability to produce extremely thin films even for reasonably large flow rates, with very short residence times. Furthermore, they require lower pumping energy than other continuous-flow mixing devices. This is because, in such devices, the liquid film does not experience any pressure drop on the surface of the disk, and the centrifugal acceleration is enough to ensure a continuous flow of the thin liquid film. Consequently, spinning disk reactors can be operated in continuous mode with less energy consumption than tubular mixers. In fact, once the disk is in motion, a relatively small amount of energy to keep the disk rotating is required, due to the high inertia exhibited by the disk. The high performance that characterizes

* To whom all correspondence should be addressed. E-mail: chianese@ingchim.ing.uniroma1.it. Tel: +39 06 44585928. Fax: +39 06 4827453.

[†] University of Rome.

[‡] University of Newcastle upon Tyne.

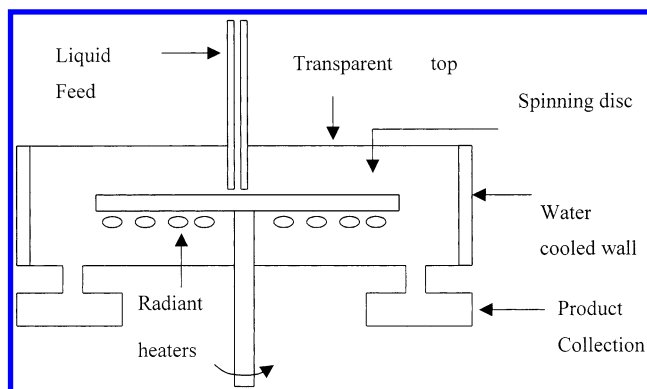


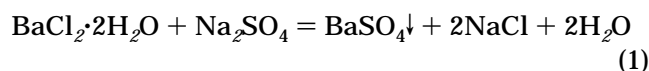
Figure 1. Schematic representation of the spinning disk reactor.

spinning disk reactors is mainly due to the high shear forces and instability that can be generated within the thin liquid films as they drain over the surface of the rotating disk. These forces give rise to waves and ripples, which enhance the intensity of mixing and the heat/mass-transfer rates produced in such reactors. In addition such reactors provide a higher surface area-to-volume ratio than the T-mixers and Y-mixers, which could reduce the frequency of collisions between precipitated particles and, hence, influence agglomeration phenomena.

In this paper, results of an experimental investigation using the spinning disk reactor technology for precipitating barium sulfate are presented. Comparison with published data on the continuous-flow mixer (T-mixer) is also shown.

Experimental Setup

In this work, the precipitation of barium sulfate corresponding to the following reaction was studied:



Precipitation experiments were carried out on a rotating disk of 0.5 m in diameter. A schematic representation of the system is shown in Figure 1. The brass disk used in the study was sprayed with aluminum bronze powder to create surface imperfections of the order of 100 μm in order to promote mixing in the liquid film. A variable-speed motor was used to operate the spinning disk, and the motor drive was connected to the bottom of the disk via a central shaft. The speed of the disk was varied by using a control regulator between 100 and 1000 rpm and was recorded by an analog tachometer. The accuracy of the tachometer was within 10 rpm. The two aqueous reagent solutions were fed onto the disk surface by means of two 56-mL burets, which were located at a radial distance of 0.05 m from the center of the disk. The precipitated slurry was collected in a vessel as shown in Figure 1.

The experiments were performed by mixing equivalent amounts of barium chloride dehydrate and sodium sulfate aqueous solutions on the surface of the spinning disk reactor. The solutions of the two reagents were not preliminarily filtered since they were fed over the disk through open air. Analytical grade chemicals were dissolved in ordinary distilled water. Experiments were carried out at 25 ± 0.5 °C. At this temperature, the equilibrium solute concentration is equal to 1.009×10^{-5}

Table 1. Number of Crystals (per cm^{-3}) at Different Levels of Supersaturation for the Spinning Disk Reactor

supersaturation level	no. of crystals/ cm^3
100	6.9×10^7
2000	3.2×10^9
2500	4.0×10^9

M. The reactant flow rates were equal to 1.33×10^{-6} m^3/s and each run lasted 86 s.

Through each run, 2 mL of the slurry was sampled at fixed time intervals, from the disk housing. After the withdrawal, the samples were quickly poured into 20 mL of 0.02 wt % gelatine solution. According to Nielsen³ and Mohanty et al.,⁴ this procedure avoids the agglomeration and settling of the particles and the dilution arrested or reduced the growth rate of crystals. Both the crystal habit and the number of particles were examined by using a transmission electron microscope and a hemocytometer, respectively.

Samples for transmission electron microscopy were prepared by introducing a few drops of the suspension into a carbon-coated copper grid (200 mesh). The grid was placed on a filter paper in order to absorb the excess solution. It was then dried to recover the crystals.

A 1-mL sample of the suspension was used in a hemocytometer for counting the number of precipitated particles. The counting cell was placed under a light microscope, which was connected to a camera, which was used to take three pictures per sample. In each photograph, six squares of the grid were distinctly visible. Thus, 18 squares/sample were used for counting.

The crystal size was evaluated by image analysis of the crystal photos made by TEM.

An X-ray diffraction analysis of the solid product was then performed. The suspension was filtered on a blue Whatman filter paper using a vacuum pump and dried in an oven at 100 °C. The dried precipitate was then bombarded by Co K α rays and was confirmed to be anhydrous BaSO_4 .

Experimental Results

The first runs were operated at a potential supersaturation ratio expressed in terms of solute concentration, S_0 , ranging between 100 and 10 000. The first series of three runs was made at a rotating speed of 1000 rpm and initial supersaturation values of 100, 2000, and 2500. The number of crystals per cubic centimeter is given in Table 1. That is, it increased as the initial supersaturation level increased. It is noted that, at an initial supersaturation value of 100, the number of precipitated crystals per cubic centimeter when the spinning disk reactor is used is 6.9×10^7 . Whereas, Nielsen,³ by using a T-mixer at the same supersaturation level, counted 5.0×10^5 crystals. Similarly, the number of crystals generated at $S_0 = 2000$, i.e., 3.2×10^9 , is significantly more than the number of crystals counted by Mohanty et al.⁴ when using a T-mixer, which ranges between 2.2×10^8 and 4.0×10^8 . Mohanty et al.⁴ emphasized that homogeneous nucleation took place in their experiments for an initial supersaturation equal or higher than 2000. Therefore, it was concluded that the number of generated particles in the runs carried out in this work at a rotational speed of 900 rpm or higher is comparable with that resulting from homogeneous nucleation for the same levels of

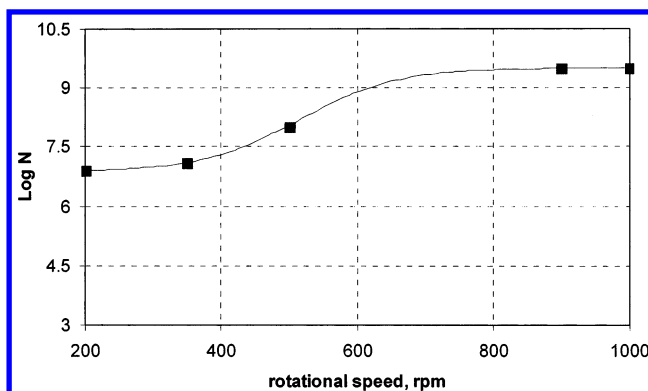


Figure 2. Particle number N per cubic centimeter versus the rotational speed for the spinning disk crystallizer. The initial supersaturation was $S_0 = 2000$.

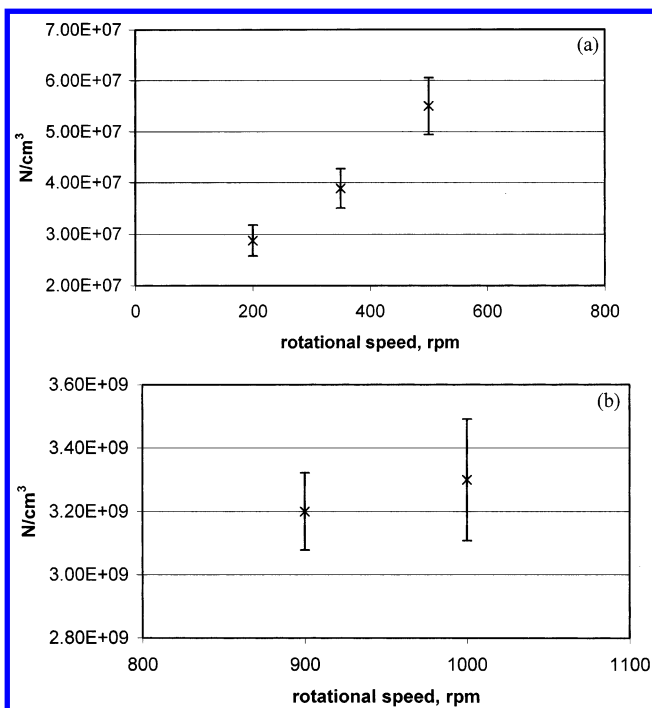


Figure 3. Particle number per cubic centimeter versus rotational speed. The bars represent the confidence interval of the measurement at 95% of probability.

initial supersaturation ($S_0 = 2000$ and $S_0 = 2500$). However, nucleation occurring in these runs is here defined as spontaneous instead of homogeneous, because it is due essentially but not exclusively to the homogeneous mechanism for the high number of foreign particles that might be present in the solution and induce heterogeneous nucleation.

Subsequently, five runs were then made at various rotation speeds in the range 200–1000 rpm, at an initial supersaturation value of 2000, to evaluate the influence of hydrodynamics on the precipitation process. The plot of the logarithm of the number of precipitated crystals against the rotational speed is given in Figure 2. The number of crystals at a rotation speed equal or higher than 900 rpm is 2 orders of magnitude greater than the number of crystals at a rotation speed equal to or less than 500 rpm. In Figure 3, the same data are reported, by using a linear Y axis, together with the bars expressing the confidence interval at 95% of probability of the number of crystal measurements. It is clear that the crystal production rate continuously increases on in-

creasing the rotation speed between 200 and 500 rpm, whereas it does not change significantly for 900 and 1000 rpm.

It was also observed that when the rotation speed is increased from 200 rpm up to 1000 rpm, the average crystal dimension decreases from 3.0 to 0.7 μm . Furthermore, at a rotation speed of 1000 rpm, the size range of the precipitated crystals was very narrow (0.5–1 μm). These results may be interpreted as a consequence of the attainment at a high rotation speed of conditions of micromixing, which enables in correspondence to high supersaturation the occurrence of homogeneous nucleation in addition to heterogeneous nucleation. Under such conditions, a high number of nuclei are generated, the supersaturation in the solution flowing away from the feed point suddenly decreases, and the final crystal size of the product is very small.

The image of the crystals produced at an initial supersaturation of 2000 and a rotation speed of the spinning disk of 500 rpm, detected by the transmission electron microscope, appeared to be monocrystals of barium sulfate and look similar to the ones produced at the same initial supersaturation by Mohanty et al.⁴ using a T-mixer with an outlet arm of 3 or 9 mm.

Discussion

The operating conditions of interest were those corresponding to an initial supersaturation level of 2000. This was attained by mixing equivalent amounts of barium chloride dihydrate and sodium sulfate solutions (0.04 M) on the surface of the spinning disk reactor.

First, the mass balance for BaSO_4 was verified in order to validate the measured number of precipitated crystals. Given that the overall inlet concentration of both ions Ba^{2+} and SO_4^{2-} was 0.02 M and the molecular mass of barium sulfate is 0.233 39 kg/mol, the inlet mass of barium sulfate per cubic centimeter of solution was $\sim 0.466\,78 \times 10^{-5} \text{ kg/cm}^3$. This was compared with the outlet mass of barium sulfate, which was calculated on the basis of the number of precipitated particles ($3.2 \times 10^9/\text{cm}^3$) and the average size of the particles (0.7 μm). In particular, denoting the volumetric shape factor by k_v , the volume of the single particle was approximated as $k_v 0.343 \times 10^{-18} \text{ m}^3$. Hence, on the basis of the density of barium sulfate (4500 kg/m³), the mass of the single particle was approximated by $k_v 1.5435 \times 10^{-15} \text{ kg}$. This, multiplying by the number of precipitated particles, gives an overall precipitated mass of barium sulfate solution equal to $k_v 0.493\,92 \times 10^{-5} \text{ kg/cm}^3$, which would be the same as the inlet mass for k_v equal to 0.945. This value of the volumetric shape factor, which appears reasonable for an almost cubic crystal, confirms the consistency of the obtained results with the mass balance.

To check whether the operating conditions are such that homogeneous nucleation predominates, the occurrence of micromixing for the spinning disk operated at $S_0 = 2000$ and rotation speed equal to 900 rpm was examined. Micromixing is defined as a very effective mixing of the two reagents at molecular level. Micromixing conditions are achieved when the mixing time, t_m , is shorter than the induction time, t_{ind} , which is the overall time required for the reaction, nucleation, and outgrowth of the generated crystals to the detectable size. In this case, the overall rate of the reaction crystallization process is not affected by the mixing intensity. It is noticed that the reaction is a very fast

process for slightly soluble salts and the time that elapses between the reaction and the nucleation is negligible; thus, the induction time can only be attributed to the nucleation and outgrowth processes.

During the experiments carried out on the spinning disk reactor, it was not possible to detect the appearance of the first precipitated particles in the liquid film flowing over the surface of the disk. Therefore, to estimate the induction time for the precipitation of barium sulfate on the spinning disk reactor, the expression determined by Carosso and Pellizzetti⁵ was adopted:

$$\text{Log}(t_{\text{ind}}) = 15.5 \text{ Log}^{-2} S_a - 4.2 \quad (2)$$

where the supersaturation ratio S_a is expressed in terms of the activity coefficients of the Ba^{2+} and SO_4^{2-} ions in solution. To identify this expression, the authors used light transmittance as a medium to measure the time of formation of the particles of barium sulfate. Such apparatus could measure induction times ranging between 30 and 5 ms. The equipment was similar to a Y-mixer, operated with concentrations of barium sulfate ranging between 8×10^{-4} and 8×10^{-3} mol/L, and the nucleation was considered to be homogeneous. With respect to this issue, it is noted that the concentration of barium sulfate used for the experiments on the spinning disk reactor (2×10^{-2} M) is higher than the concentration used by Carosso and Pellizzetti.⁵ Nevertheless, the approximation due to the use of eq 2 to extrapolate the induction time for the homogeneous nucleation of barium sulfate on the spinning disk was considered acceptable since homogeneous nucleation is only dependent on temperature and independent of the setup geometry.

The calculation of the supersaturation level in terms of the activity coefficients was carried out following Söhnel and Garside⁶ and using, in particular, the Bromley correlation for multicomponent systems (expressions 2.60–2.64⁶). This gave an activity coefficient γ that is approximately equal to 0.31 for the 0.02 M barium sulfate solution, with supersaturation expressed in terms of the activity coefficients, S_a , equal to 1272. Using eq 2, the corresponding induction time, t_{ind} , is approximately equal to 2.56 ms. The mixing time, t_m , of the reactant solutions on the spinning disk was calculated on the basis of the hydrodynamic properties of the aqueous solution and of the specific dispersed power, ϵ , referred to the whole active disk surface. This was estimated following Moore:⁷

$$t_m = 2(\nu_L/\epsilon) \arcsin(0.05Sc) \quad (3)$$

where ν_L denotes the kinematic viscosity of the solvent. Sc is the Schmidt number given by

$$Sc = \nu_L/D \quad (4)$$

where D denotes the diffusion coefficient. For the case study examined in this work, the kinematic viscosity, ν_L , is equal to 1.022×10^{-6} (m²/s), the diffusion coefficient, D , is equal to 9.42×10^{-9} (m²/s), and the Schmidt number, Sc , is equal to 108.59.

Following Moore,⁷ the specific dispersed power, ϵ , in eq 3, was computed as

$$\epsilon = (1/2t_{\text{res}})\{(r^2\omega^2 + u^2)_o - (r^2\omega^2 + u^2)_i\} \quad (5)$$

where t_{res} denotes the residence time of the liquid

solution on the spinning disk, r the radial distance from the center of the disk, ω the angular velocity of the disk, and u the average velocity of the liquid solution on the disk. In eq 5, the subscripts “o” and “i” indicate whether r , ω , and u must be computed on the outer or inner radius of the disk, respectively.

The average velocity, u , of the liquid solution on the disk is given by

$$u = (\rho_L Q_L^2 \omega^2 / 12\pi^2 \mu_L r)^{1/3} \quad (6)$$

where Q_L denotes the flow rate on the disk, ρ_L the density of the solution, and μ_L the viscosity of the solvent.

The residence time of the solution on the disk was calculated as

$$t_{\text{res}} = \frac{3}{4}(12\pi^2)^{1/3} \left[\frac{\mu_L(r_o^4 - r_i^4)}{\rho_L \omega^2 Q_L^2} \right]^{1/3} \quad (7)$$

For the adopted disk, the inner radius was 0.10 m, corresponding to the feed point, and the outer radius was 0.25 m. Thus, for a supersaturation value of 1272, at a rotational speed of 900 rpm, (with a residence time of ~2.31 s) the specific dispersed power is 115 W/kg, and the mixing time is shorter than 0.9 ms, which is significantly shorter than the induction time computed with eq 2, i.e., 2.56 ms. A value of ~1 ms for the mixing time was also reported by Nielsen.⁸ In case nucleation does not take place over the whole disk, but only on a part of it, the specific dispersed power decreases, but it is always of the order of milliseconds. For instance, if nucleation takes place only over 20% of the area of the disk, that is, between the inner diameter equal to 0.100 m and a diameter equal to 0.143 m, the specific dispersed power becomes equal to 53 W/kg and the mixing time is equal to 1.9 s, thus still lower than the induction time.

The knowledge of the specific dispersed power allows the determination of the Kolmogoroff turbulent microscale λ_k , expressed as

$$\lambda_k = \sqrt[4]{(\nu_L/\sigma_L)\epsilon} \quad (8)$$

This microscale is a measure of the turbulent eddy size. The effectiveness of micromixing is inversely proportional to the Kolmogoroff microscale. For the spinning disk operating at 900 rpm, a value of $\lambda_k \cong 10 \mu\text{m}$ can be estimated. It is necessary to observe that λ_k should be evaluated from the local and not from the average energy dissipation. However, on the basis of the above calculations and the obtained results, it is possible to conclude that for the precipitation of barium sulfate occurring over the spinning disk a Kolmogoroff turbulent microscale equal or lower than $10 \mu\text{m}$ leads to spontaneous precipitation.

The calculated values of t_m and t_{ind} confirm the experimental results. In fact, by increasing the rotational speed of the spinning disk, it is possible to attain a micromixing time in the liquid film on the surface of the disk shorter than the induction time and operating conditions for the occurrence of homogeneous nucleation.

A further validation of the nucleation results was made on the basis of the comparison of the theoretical (ideal) nucleation rate, computed following Söhnel and Garside,⁶ with the experimental nucleation rate, com-

puted on the basis of the number of precipitated particles and the mixing time. The theoretical nucleation rate was found equal to $2.48 \times 10^{13} \text{ cm}^{-3} \text{ s}^{-1}$ (see Appendix). The experimental nucleation rate was computed on the basis of the number of precipitated particles per cubic centimeter (3.2×10^9) and the induction time (2.59 ms), and it was found to be $\sim 1.25 \times 10^{12} \text{ cm}^{-3} \text{ s}^{-1}$, which is fairly consistent with the theoretical value.

Finally, a comparison was carried out on the specific dispersed power used in the spinning disk reactors and in the traditional T-mixers and Y-mixers.^{4,9,10} These devices provide a direct mixing of the feed streams together in a very small volume, which enhances the mixing conditions and ensures very low micromixing times (less than 10 ms). Furthermore, because of the small volume in which the reactants mix, very high levels of supersaturation are reached in a well-defined and relatively small area of the reactor, making the precipitation process easier to control. In fact, as observed by Bénét et al.,¹¹ in continuous-flow mixers, the level of supersaturation at which the nucleation process takes place is much more related to the initial reactant concentration than it is in stirred tank reactors. The geometry of these devices and the flow conditions prevent the occurrence of backmixing and recirculation phenomena. In addition, a sudden drop of the supersaturation level in the outlet conduct reduces secondary nucleation and crystal growth phenomena.¹⁰ Therefore, the main advantage derived from using such devices is that the precipitation of primary particles can be controlled by the initial supersaturation.

However, it is noted that, because of their design, continuous-flow mixers exhibit an intense pressure drop in the mixing chamber. Consequently, operation of such devices requires a very high specific power input, which is generally of the order of 100 kW/kg. In particular, the results attained on the spinning disk were compared with those published by Mohanty et al.⁴ for a T-mixer with an arm of 9 mm, at $N_{Re} = 24\,000$, and a measured pressure drop of 310 kPa. The specific dispersed power for this configuration of the T-mixer was evaluated on the basis of the pressure friction drop in the mix chamber of the T geometry,¹² which was estimated to be equal to 80 kPa. Then, by using the expression reported by Mohanty et al.:⁴

$$\epsilon = \frac{\Delta p Q_L}{\rho_L (\pi d^5/4) L} \quad (9)$$

the specific dispersed power was found equal to $\sim 112 \text{ kW/kg}$. This value was found to be in accordance with the references found in the literature.^{9,11} For the same T-mixer geometry, the micromixing time was calculated using the relationship proposed by Geisler:¹³

$$t_m = 50(\nu_L/\epsilon)^{1/2}(0.88 + \ln(Sc)) \quad (10)$$

and was found to be equal to $\sim 1.05 \text{ ms}$, which is in accordance with the mixing time estimated by Mohanty et al.⁴

In Table 2, spinning disk reactors and T-mixers are compared in terms of the number of crystals per cubic centimeter, dispersed specific power, and mixing time. From this table it is evident that the spinning disk reactor can provide an intense mixing at a significantly lower power dispersion than the T-mixer. In particular,

Table 2. Comparison of Spinning Disk Reactor and T-Mixer. Results for Initial Supersaturation of 2000

	T-mixer ⁴	spinning disk (900 rpm)
no. of crystals/cm ³	$(2-4) \times 10^8$	4×10^9
specific dispersed power (w/kg)	100×10^3	115
mixing time (ms)	1.05	0.9

although the number of crystals per cubic centimeter precipitated by means of the two techniques is similar, the specific dispersed power for the spinning disk reactor is significantly lower than the specific dispersed power for the rapid T-mixer. Consequently, it can be argued that spinning disk reactors represent valid candidates for the industrial application of precipitation processes with a very high nucleation rate. Furthermore, the scale-up to industrial scale of such devices is not as problematic as the scale-up of rapid T-mixers and Y-mixers. This is mainly due to the fact that spinning disk reactors do not appear to be prone to incrustation problems and do not exhibit the extreme pressure drops that are typical of tubular T-mixers and Y-mixers. As a consequence, it is feasible to operate such reactors in continuous mode with a significantly small power consumption.

It also needs to be mentioned that the high supersaturation level and the intense mixing conditions confined in a very small area enhance agglomeration phenomena between the precipitated particles and incrustation in the conduct of T-mixers and Y-mixers. Furthermore, agglomeration phenomena, apart from degrading the quality of the product, may imply changes in the rheological properties of the suspension,¹⁰ which can then increase the pressure drop in the mixing chamber. These problems impose severe limitations to the scale-up of T-mixers and Y-mixers to industrial scale. To overcome this limitation, Bénét et al.¹¹ proposed a boundary free continuous-flow mixer. This is constituted of a two-impinging jets (TIJ) mixer immersed in a stirred tank reactor. The authors claim mixing times of up to 2 ms, i.e., comparable to the mixing time of T-mixers and Y-mixers. Nevertheless, the problem of high specific power consumption remains. In addition to the ability of the SDR to promote very high nucleation with reduced power consumption, it offers the following opportunities: coating of particles as they are formed by introducing a third stream on the disk and carrying out precipitation reactions at controlled temperatures due to the good heat-transfer characteristics of SDRs. The ease with which the disk surface can be cleaned and the fact that these reactors can be designed to include nonevasive analytical techniques for product characterization makes this concept of processing quite attractive.

Conclusions

Homogeneous nucleation of primary particles represents an appealing methodology for the production of nanosize particles. Intense mixing conditions, with micromixing times shorter than the induction time of the precipitation reaction, are required to enhance homogeneous nucleation of primary particles. It is known that stirred tank reactors cannot provide the required intense local mixing conditions and uniform level of supersaturation in the reactors. On the other hand, continuous-flow mixers, such as T-mixers and Y-mixers, have been shown to provide such conditions.

However, this is achieved with a significant power dissipation (of the order of 100 kW/kg). This, in conjunction with severe incrustation problems, makes the scale-up to an industrial scale of such devices unfeasible. Spinning disk reactors are known to provide the intense mixing conditions that are required for homogeneous nucleation of primary particles. Such reactors have been successfully used as polymerization reactors and in general for intensified heat-transfer processes.

In this work, the use of a spinning disk reactor is proposed in order to accomplish the precipitation of barium sulfate. By operating a smooth disk (0.5 m in diameter) at a rotation speed of 900–1000 rpm, experimental results were obtained in good agreement with those found in the literature, concerning the use of a rapid T-mixer. In particular, with a specific dispersed power of 115 W/kg, it was possible to produce a very high specific number of crystals in the size range 0.5–1 μm . The comparison of the induction and mixing time confirmed that at the adopted operating conditions homogeneous nucleation may occur. From these results, spinning disk reactors appear to be valuable equipment for carrying out a reaction–precipitation process.

Appendix

The dimensionless driving force for the nucleation process is

$$-(\Delta\mu_i/RT) = \ln(a/a^*) \quad (11)$$

the superscript “*” refers to the equilibrium or saturation. If the dissolved component is an electrolyte that dissociates in solution to give ν_+ cations and ν_- anions, the activity can be expressed as

$$a = a_{\pm}^{\nu} = (Qm\gamma_{\pm})^{\nu} \quad (12)$$

where m is the concentration expressed in molality, γ_{\pm} the mean ionic activity coefficient, $Q = (\nu_+^{\nu_+}\nu_-^{\nu_-})^{1/\nu}$, and $\nu = \nu_+ + \nu_-$. By including the activity expression given by eq 12 in eq 11 the crystallization driving force becomes

$$-(\Delta\mu/RT) = \ln(a_{\pm}/a_{\pm}^*)^{\nu} = \nu \ln S_a = \nu \ln S_0 \xi_c \quad (13)$$

where $S_a = a_{\pm}/a_{\pm}^*$, $S_0 = d/c^*$, $\xi_c = \gamma_{\pm}/\gamma_{\pm}^*$, S_a and S_0 represents the definition of supersaturation in terms of activity and concentration, respectively.

The energy barrier to nucleation corresponds to the change of Gibbs energy accompanying formation of the critical nucleus. In the case of homogeneous nucleation, this energy change is given by:

$$\Delta G_{\text{hom}}^* = \beta \nu^2 \gamma^s / \phi^2 \quad (14)$$

where β denotes the geometric factor, which can be written as

$$\beta = 4k_a^3/27k_v^2 \quad (15)$$

and for barium sulfate, assuming a cubic crystal, $k_a = 6$ and $k_v = 1$, hence $\beta = 32$. In eq 14, ν is the molecular volume given by

$$\nu = M/\rho_s N_A \quad (16)$$

where, for barium sulfate, the molecular mass M is

equal to 233.39 g/mol and the density ρ_s is equal to 4500 kg/m³ ($N_A = 6.023 \times 10^{23}$). Thus, the molecular volume is equal to 8.60×10^{-29} m³. In eq 14, γ^s is the surface energy, which is equal to 0.136 J/m², and ϕ denotes the reaction affinity given by

$$\phi = \nu kT \ln(S_a) \quad (17)$$

which, from example 3.1 in Söhnel,⁶ with a supersaturation $S_a = 1272$, is equal to 5.87×10^{-20} J. The calculation of the supersaturation level in terms of the activity coefficients, S_a , was carried out following Söhnel⁶ and using, in particular, the Bromley correlation for multicomponent systems (expressions 2.60–2.64, in ref 6).

The nucleation rate J can then be expressed as

$$J = \Omega \exp(-(\Delta G_{\text{hom}}^*)/kT) \quad (18)$$

where the preexponential term Ω can be computed as

$$\Omega = \frac{5.99 \times 10^{37}}{N^*} \left[\frac{4\Delta G_{\text{hom}}^*}{3\pi kT} \right]^{1/2} \quad (19)$$

from Söhnel⁶ and the number of molecules N^* forming the critical nucleus given by

$$N^* = \beta \nu^2 \gamma^s / \phi^3 \quad (20)$$

is equal to 5.87. Thus, Ω is equal to 4.28×10^{37} . And, according to eq 11, the theoretical nucleation rate J is equal to 2.48×10^{13} cm⁻³ s⁻¹.

Nomenclature

- a = activity
- a_i = activity of component i in solution
- c = concentration of barium sulfate in solution
- c^* = equilibrium concentration of barium sulfate in solution
- D = diffusion coefficient
- d = inner diameter T-mixer arm
- ΔG = Gibbs energy change
- i = inner side of the disk
- J = nucleation rate
- k_v = volumetric shape factor
- L = length of T-mixer arm
- m = molality
- M = molecular mass of barium sulfate
- N^* = number of molecules forming the critical nucleus
- o = outer side of the disk
- p = pressure
- Δp = pressure drop
- Q_L = liquid flow rate
- Q = geometric average of ions in solution, $Q = (\nu_+^{\nu_+} \nu_-^{\nu_-})^{1/\nu}$
- r = radial distance from the center of the disk
- S_a = supersaturation ratio expressed in terms of activity coefficients
- Sc = Schmidt number
- S_0 = supersaturation ratio expressed in terms of concentrations
- t_m = mixing time
- t_{ind} = induction time
- t_{res} = residence time
- u = average velocity of the liquid solution on the disk
- ν = molecular volume

Greek Symbols

- β = shape factor
- γ_{\pm} = mean ionic activity
- γ = activity coefficient

γ^s = surface energy
 ϵ = specific dispersed power
 ϕ = reaction affinity
 λ_k = Kolmogoroff turbulent microscale
 μ_L = viscosity of the solvent, chemical potential
 $\Delta\mu$ = variation of chemical potential
 ν_L = kinematic viscosity
 ν_+ = cations in solution
 ν_- = sum of anions in solution
 ν = ions in solution, $\nu = \nu_+ + \nu_-$
 ρ_L = density of the solution
 ρ_s = density of the solute
 ω = angular velocity of the disk
 Ω = preexponential term for nucleation rate

Literature Cited

- (1) Jachuck, R. J. J.; Ramshaw, C. Process Intensification: Heat Transfer Characteristics of Tailored Rotating Surfaces. *Heat Recovery Syst., CHP* **1994**, 14 (5), 475.
- (2) Boodhoo, K.; Jachuck, R., J., J. Process Intensification: Spinning Disc Reactor for Styrene Polymerisation *Appl. Therm. Eng.* **2000**, 20, 1127.
- (3) Nielsen, A. E. Homogeneous Nucleation in Barium Sulphate Precipitation. *Acta Chem. Scand.* **1961**, 15, 441.
- (4) Mohanty, R.; Bhandarkar, S.; Zuromski, B.; Brown, R.; Estrin, J. Characterizing the Product Crystals from a Mixing Tee Process. *AIChE J.* **1988**, 34 (12), 2063.
- (5) Carosso, P. A.; Pellizzetti, E. A Stopped-Flow Technique in Fast Precipitation Kinetics. The Case of Barium Sulphate. *J. Cryst. Growth* **1984**, 68, 532.
- (6) Sönhel, O.; Garside, J. *Precipitation, Basic Principles and Industrial Applications*; Butterworth-Heinemann Ltd.: Oxford, U.K., 1992.
- (7) Moore, S. R. Mass Transfer to Thin Liquid Films on Rotating Surfaces, with and without Chemical Reaction, Ph.D. Dissertation, University of Newcastle upon Tyne, Newcastle upon Tyne, U.K., 1996.
- (8) Nielsen, A. E. Nucleation and Growth of Crystals at High Supersaturation. *Krist. Tech.* **1969**, 4, 17.
- (9) Heyer, C.; Mersmann, A. The Influence of Operating Conditions on the Precipitation of Nanoparticles. 14th International Symposium on Industrial Crystallization, Cambridge, September 1999; Poster 153.
- (10) Kind, M. Precipitation Phenomena and their Relevance to Precipitation Technology. 14th International Symposium on Industrial Crystallization, Cambridge, September 1999; Plenary Lecture P1.
- (11) Bénet, N.; Flak, L.; Muhr, H.; Plasari, E. Experimental Study of a Two-Impinging-Jet Mixing Device for Application in Precipitation Processes. 14th International Symposium on Industrial Crystallization, Cambridge, September 1999; Poster 10.
- (12) Glück, B. *Hydrodynamische und gasdynamische Rohrströmung: Druckverluste*; VEB Verlag für Bauwesen: Berlin, 1988.
- (13) Geisler, R.; Mersmann, A.; Voit, H. Makro- und Mikromische im Rührkessel. *Chem. Ing. Tech.* **1988**, 60, 947.

Received for review August 3, 2001

Revised manuscript received April 26, 2002

Accepted August 6, 2002

IE010654W